



Published in final edited form as:

Brain Res. 2017 February 15; 1657: 148–155. doi:10.1016/j.brainres.2016.11.024.

Disruption of a putative intersubunit electrostatic bond enhances agonist efficacy at the human $\alpha 1$ glycine receptor

Brian T. Welsh^d, Jelena Todorovic^c, Dean Kirson^d, Hunter M. Allen^c, Michelle D. Bayly^d, and S. John Mihic^{a,b,c,d,e,*}

^aDepartment of Neuroscience, University of Texas at Austin, Austin, Texas 78712

^bDivision of Pharmacology and Toxicology, University of Texas at Austin, Austin, Texas 78712

^cWaggoner Center for Alcohol & Addiction Research, University of Texas at Austin, Austin, Texas 78712

^dInstitutes for Neuroscience, University of Texas at Austin, Austin, Texas 78712

^eCell & Molecular Biology, University of Texas at Austin, Austin, Texas 78712

Abstract

Partial agonists have lower efficacies than compounds considered ‘full agonists’, eliciting submaximal responses even at saturating concentrations. Taurine is a partial agonist at the glycine receptor (GlyR), a member of the cys-loop ligand-gated ion channel superfamily. The molecular mechanisms responsible for agonism are not fully understood but evidence suggests that efficacy at these receptors is determined by conformational changes that occur early in the process of receptor activation. We previously identified a residue located near the human $\alpha 1$ glycine binding site (aspartate-97; D97) that, when mutated to arginine (D97R), results in GlyR channels opening spontaneously with a high open probability, mimicking the effects of saturating glycine concentrations on wildtype GlyR. This D97 residue is hypothesized to form an electrostatic interaction with arginine-119 on an adjacent subunit, stabilizing the channel in a shut state. Here we demonstrate that the disruption of this putative bond increases the efficacy of partial agonists including taurine, as well as two other β -amino acid partial agonists, β -aminobutyric acid (β -ABA) and β -aminoisobutyric acid (β -AIBA). Even the subtle charge-conserving mutation of D97 to glutamate (D97E) markedly affects partial agonist efficacy. Mutation to the neutral alanine residue in the D97A mutant mimics the effects seen with D97R, indicating that charge repulsion does not significantly affect these findings. Our findings suggest that the determination of efficacy following ligand binding to the glycine receptor may involve the disruption of an intersubunit electrostatic interaction occurring near the agonist binding site.

*Corresponding Author: S. John Mihic, Ph.D., Department of Neuroscience, MC A4800, 2500 Speedway, University of Texas at Austin, Austin, TX 78712, Phone: 512-232-7174, FAX: 512-232-2525, mihic@austin.utexas.edu.

Publisher's Disclaimer: This is a PDF file of an unedited manuscript that has been accepted for publication. As a service to our customers we are providing this early version of the manuscript. The manuscript will undergo copyediting, typesetting, and review of the resulting proof before it is published in its final citable form. Please note that during the production process errors may be discovered which could affect the content, and all legal disclaimers that apply to the journal pertain.

Keywords

Partial agonist; Efficacy; Taurine; Glycine receptor; Single channel; Electrophysiology

1. Introduction

The glycine receptor (GlyR), expressed throughout the nervous system, is a member of the Cys-loop ligand-gated ion channel superfamily. Most GlyR in adults are composed of $\alpha 1\beta$ heteromers, but $\alpha 1$ subunits can also form functional homomeric receptors in many expression systems (Kuhse et al., 1995). Glycine is thought to be the endogenous ligand for synaptic GlyR, but evidence exists that taurine tonically activates extrasynaptic GlyR (Mori et al., 2002). Taurine concentrations in mammalian cerebrospinal fluid are typically 10–100 μM , and in rats are particularly high in the cerebral cortex, olfactory bulb and cerebellum (Huxtable, 1992); GlyR expression has been noted in all these brain regions (Lynch, 2004). For example, taurine may be acting as an endogenous ligand at GlyR to increase dopamine release in the nucleus accumbens, a brain region implicated in reward (Ericson et al., 2006). Taurine efficacy varies substantially depending on the expression system and GlyR subunit composition. Taurine most often acts as a partial agonist, yielding currents that are 5 – 60% in magnitude relative to the effects produced by maximally-effective concentrations of glycine. These effects are seen in homomeric $\alpha 1$ and $\alpha 2$ GlyR, and heteromeric $\alpha 1\beta$ and $\alpha 2\beta$ GlyR expressed in basolateral amygdala neurons (McCool and Botting, 2000), HEK 293 cells (Lape et al., 2008), and *Xenopus* oocytes (Schmieden et al., 1999).

The GlyR is pentameric, with each subunit consisting of an extracellular ligand binding domain (LBD), four transmembrane (TM) segments, and a large intracellular loop between TM3 and TM4. Binding of neurotransmitter produces conformational changes that are rapidly transmitted to the membrane-spanning pore, ultimately opening the ion channel. Previously we showed that mutation of the aspartate-97 residue to arginine (D97R) in loop A in the LBD of the $\alpha 1$ subunit favors spontaneous transitions of channels to the open state (Beckstead et al., 2002). Subsequently we found that this spontaneous activity was due to the disruption of a putative intersubunit electrostatic bond involving D97 and at least R119 of an adjacent subunit (Todorovic et al., 2010). Single channel recordings showed that clusters of spontaneous D97R GlyR openings had a P_{open} of 0.91, very similar to that observed when wildtype $\alpha 1$ GlyR are exposed to saturating concentrations of glycine. A high P_{open} of 0.96 is also observed in $\alpha 1\beta$ GlyR exposed to saturating glycine concentrations; however these receptors exhibit a P_{open} of 0.54 in response to a maximally-effective concentration of taurine (Lape et al., 2008). We thus hypothesized that the efficacy difference between glycine and taurine might be partially due to differences in their abilities to break this intersubunit electrostatic bond in wildtype GlyR, and that in mutated receptors, in which this bond is broken, the efficacy of taurine would increase. Lape et al (2008) suggested that the efficacies of agonists and partial agonists in the nicotinic acetylcholine receptor superfamily are defined by transitions from a closed state to an intermediate closed state (flipped) that follows ligand binding but precedes channel opening. According to this model, efficacy is determined by the rates governing the transitions between closed and flipped states, as well as transitions between flipped and open. One conclusion reached by

the authors was that the determination of whether a compound acts as a partial or full agonist occurs early in the process of receptor activation. In the present report we focus on the D97 residue, which is positioned in the ligand binding domain to play a role in the initial steps of receptor activation.

2. Results

2.1 – Mutation of residue 97 to D97R increases taurine efficacy

Oocytes were injected with WT or mutant $\alpha 1$ GlyR subunits in order to compare their responses to agonists varying in efficacy. Perfusion of either 10 mM glycine or 100 mM taurine produced robust inward currents on WT GlyR, with taurine eliciting $41 \pm 4.5\%$ of the maximal current produced by glycine in the same oocyte (Figs. 1A and B). However, on the D97R GlyR maximal taurine and glycine responses were approximately equal (Figs. 1C and D). In the WT receptor, the EC_{50} of glycine was 316 μ M while the taurine EC_{50} was 1.96 mM (Fig. 1B). The D97R mutation reduced the potencies of both glycine and taurine, with EC_{50} s of 760 μ M and 10.5 mM respectively (Fig. 1D). Zinc is an endogenous GlyR modulator found at concentrations in buffer solutions sufficient to affect receptor function (Cornelison and Mihic, 2014). To prevent contributions of contaminating zinc to the measured efficacies of these agonists, all solutions contained 2.5 mM tricine to chelate free zinc (Miller et al., 2008). In addition, glycine contamination of saturating taurine stock solutions was found to be sufficiently high by Lape et al. (2008), at 3 parts per 100,000, to affect their single channel kinetic modeling. We determined that co-application of 10 – 100 μ M glycine with 100 mM taurine did not enhance whole-cell currents, compared to those produced by taurine alone (Supplementary Fig. 1); small contaminating concentrations of glycine do not significantly affect the GlyR responses we observed in the presence of taurine.

2.2 – D97R single channel responses in absence and presence of ligands

Figure 2A shows single channel tracings obtained from an outside-out patch pulled from oocytes expressing D97R receptors. In the absence of ligand and contaminating Zn^{2+} , the D97R receptor displayed spontaneous channel openings grouped into clusters of activity separated by sojourns into what are likely desensitized states. These clusters had a P_{open} of 0.949 ± 0.004 and exhibited the same behavior as first described by Todorovic et al. (2010). When saturating concentrations of taurine or glycine were applied, the P_{open} of the clusters increased slightly to 0.990 ± 0.002 and 0.990 ± 0.001 , respectively (Figs. 2B & 2C). Open and shut dwell time distributions (Fig. 3) were fit with three exponential functions. Neither open nor shut dwell time distributions (τ s) changed appreciably in the presence of taurine or glycine (Figs 3B & 3E). A decrease in the likelihood of opening to the shortest-lived open state was observed in the presence of either taurine or glycine (Fig. 3C), but no differences were noted in shut time likelihoods (Fig. 3F). As expected, the conductance of the openings remained unchanged in the presence of taurine or glycine and was approximately 75 pS. Also as expected, taurine had a much lower P_{open} of 0.62 ± 0.06 on wildtype $\alpha 1$ GlyR, as illustrated in the tracing in Supplementary Fig. 2.

2.3 – Conservative D97E mutant retains high taurine efficacy

To test whether the increase in agonist efficacy was due specifically to the positive charge introduced at the D97 position, a conservative mutation at this residue was tested. In receptors containing the negative charge-conserving glutamate mutation at D97 (D97E), a saturating concentration of taurine still produced a current that was $95.6 \pm 4.7\%$ that of the current produced by maximally-effective glycine (Fig. 4). Like D97R, the D97E receptor exhibited strychnine-sensitive spontaneous channel opening activity.

2.4 – D97R and D97E mutations also increase β -ABA and β -AIBA efficacy

β -aminobutyric acid (β -ABA) and β -aminoisobutyric acid (β -AIBA) are also partial agonists of the WT GlyR and both have lower efficacies than taurine (Schmieden and Betz, 1995). We confirmed this in our studies demonstrating that β -ABA- and β -AIBA-induced maximal currents were $17.3 \pm 9.2\%$ and $15.3 \pm 3.3\%$ of those produced by a saturating concentration of glycine, respectively. The D97R mutation increased β -ABA- and β -AIBA-elicited maximal currents four- to five-fold, indicating that the effect of this mutation to increase the efficacy of a β -amino acid is not specific to taurine. In the case of β -ABA (Fig. 5A) the maximal currents increased to 89% of those of glycine, while β -AIBA-induced currents (Fig. 5B) increased to 61%. We also compared β -ABA and β -AIBA on D97E receptors. These receptors, like the D97R $\alpha 1$ GlyR are spontaneously active, displaying a whole-cell holding current of 264 ± 49 nA, significantly higher than the 67 ± 12 nA holding currents that are seen in WT GlyR [$t(18)=3.2$, $p<0.01$]. We reasoned that the conservative D97E mutation might retain some electrostatic interaction with R119 on an adjacent subunit, unlike the D97R charge-reversal mutation, thus limiting the efficacies of β -ABA- and β -AIBA. Interestingly β -ABA and β -AIBA appeared to act on D97E GlyR similarly to their effects on D97R receptors (Fig. 5).

2.5 – GlyR possessing a neutral D97A mutation retains high taurine efficacy

We next tested the neutral D97A mutant that possessed neither repulsive nor attractive properties in relation to R119, unlike the positively-charged D97R and negatively-charged D97E mutants. This D97A mutant was first used to demonstrate that these channels were opening spontaneously rather than being continuously open; i.e. a spontaneously-opening channel cycles among open, closed and desensitized states. Figure 6 is illustrative of this phenomenon, showing a sample tracing of a patch containing multiple D97A $\alpha 1$ GlyR. Before the application of glycine one sees the current produced by one to five channels opening spontaneously. However, not all channels that are capable of activation are open at all times since application of 10 mM glycine leads to a marked increase in current, reflecting the opening of up to 12 channels simultaneously. This demonstrates that some of these D97A $\alpha 1$ GlyR are present in a shut state capable of activation upon ligand binding. Continued application of glycine leads to desensitization, as demonstrated by the sequential closure of individual ion channels over time (Fig. 6). Single channel tracings of D97A GlyR activity in the absence and presence of taurine or glycine (Fig. 7), showed responses similar to those observed with the D97R mutant. In the absence of ligand and contaminating Zn^{2+} , the D97A receptor displayed spontaneous channel openings grouped into clusters of activity. These clusters had a P_{open} of 0.952 ± 0.006 (Fig. 7A); when saturating concentrations of

taurine or glycine were applied, the P_{open} of the clusters were 0.987 ± 0.003 and 0.938 ± 0.044 , respectively (Figs. 7B & 7C).

Open and shut dwell time distributions obtained from D97A $\alpha 1$ GlyR (Fig 8) were fit with three exponential functions. Neither open nor shut dwell time distributions (τ s) changed appreciably in the presence of taurine or glycine (Figs. 8B& 8E). Glycine produced a greater likelihood of the channel adopting the shortest-lived shut state than did taurine, but a lower likelihood of adopting the second shut state (Fig. 8F).

3. Discussion

Historically, efficacy at ion channels has been defined by the ratio of transitions to and from the open state of the channel ($E = \beta/\alpha$), where β describes the transition rate from the shut to open state of the channel and α describes the closing rate. There is thus no upper bound on efficacy, and so compounds described as ‘full agonists’ are simply those with the highest efficacy found to date, with partial agonists possessing lower efficacy. The remarkable complexity of ligand-gated ion channel structures suggests that ligand binding initiates a multitude of protein conformations, ultimately leading to channel opening. For the acetylcholine receptor, this process was mapped and the gating of the receptor was described as a Brownian conformational wave that begins in the extracellular portion of the receptor at the LBD and proceeds to the pore (Grossman et al., 2000; Auerbach, 2005).

In the present report we focused on the D97 residue, which is well positioned in the LBD to play a role in receptor activation. This amino acid is conserved across the entire cys-loop subunit superfamily, residing at a subunit interface near residues previously implicated in ligand binding (Brejc, 2001). Our previous work strongly suggested that D97 forms an intersubunit electrostatic bond with R119 (Todorovic et al., 2010), a residue earlier shown to play a role in determining glycine affinity (Grudzinska et al., 2005). In our previous study we engineered cysteine mutations at the D97 and R119 positions, and used those to show that receptor function could be markedly affected by addition of oxidizing, cross-linking or reducing agents (Todorovic et al., 2010). This strongly suggests that these two residues are close enough together to be capable of forming intersubunit disulfide bonds. However, not all evidence fully supports this assertion. D97 and R119 are 6.87 \AA apart in the zebrafish (3JAD) strychnine-bound $\alpha 1$ GlyR crystal structure (Du et al., 2015), and the equivalent residues in the human (5CFB) strychnine-bound GlyR $\alpha 3$ structure are 6.67 \AA apart (Huang et al., 2015). Charged residues 4 \AA apart or closer are interpreted as interacting electrostatically (Kumar and Nussinov, 2002). Unfortunately, to date no unliganded GlyR structures have been determined, and so it is not known how far apart these two amino acids are when no ligand has bound. Interestingly, in the zebrafish (3JAE) glycine-bound $\alpha 1$ GlyR structure (Du et al., 2015), the D97 and R119 residues are found 9.45 \AA apart, consistent with our hypothesis that agonist binding helps break this putative salt bridge.

We noticed that the spontaneous openings of the D97R $\alpha 1$ GlyR appeared to be quite similar to those elicited by a maximally-effective glycine concentration on wildtype GlyR; both generated similar open and shut dwell-time histograms, both exhibited openings grouped into clusters with P_{open} values greater than 0.9 and in both, clusters of channel-opening

events appeared to conclude with either desensitization or deactivation (Todorovic et al., 2010). We reasoned that since the breakage of the D97–R119 electrostatic bond would be consistent with clusters of spontaneous activity with a very high P_{open} , this breakage could represent an important initial step in determining an agonist's efficacy.

D97 mutant GlyR can be found in three major classes of states: those that are spontaneously open, those that are found in a shut but activatable state and those in a desensitized state, all of which are illustrated in the tracing shown in Fig. 6. Spontaneous channel opening results in whole-cell holding currents typically between 300–500 nA in magnitude, increasing to 3000–5000 nA in the presence of saturating concentrations of glycine or taurine. Since spontaneously-opening individual D97 mutant channels exhibit intra-burst P_{open} values of ~0.95 (Figs. 2A & 7A) it is inconceivable that the currents observed after applying agonists are due to an increase in the channel P_{open} of these already activated channels and must instead be due to the activation of channels that were previously in the shut state, as exemplified by the large vertical deflection in current seen in Fig. 6 when glycine is applied. This suggests that the breakage of the putative D97–R119 electrostatic bond would not be the sole determinant of channel opening, but the loss of this intersubunit interaction could decrease the energy barrier that must be surmounted in order for channels to open. Individual D97 mutant GlyR may thus open spontaneously or remain in a shut state until either glycine or taurine bind. Interestingly, even the conservative mutation to E97, differing from D97 by only a methyl group, led to channels which exhibited some spontaneous activity as well as an increased relative efficacy of taurine. This suggests the possibility that charge is not the sole factor determining the nature of an interaction between the 97 and 119 residues, and that molecular volumes or shapes of the two amino acids may also play a role.

The binding regions for glycine and taurine overlap in the $\alpha 1$ homomeric receptor (Schmieden et al., 1992) and, in particular, the I111 residue is involved in taurine activation. For example, mutations of amino acids (104, 108, and 112) near I111 enhanced the efficacy of β -amino acids (Schmieden et al., 1999). Taurine and β -ABA displayed significantly increased efficacies in these three mutants while efficacy for β -AIBA was enhanced to a lesser degree (Fig. 5). Even the conservative D97E mutation leads to greatly enhanced taurine efficacy (Fig. 4). This supports the idea that ligand efficacy is exquisitely sensitive to an electrostatic interaction involving D97. One possible explanation is that ligands could be acting as partial agonists on wildtype GlyR because they are not as effective as glycine in breaking the D97–R119 bond and this idea is supported by the crystal structure data showing that D97 and R119 are located further apart when glycine is bound than when strychnine is bound (Du et al., 2015). In mutants, this bond would be expected to be weaker or absent, thereby enhancing likelihoods of channel activation and increasing the relative efficacies of partial agonists. It should be noted that mutations at D97 also decrease agonist potency (Table 1), which is not surprising given that the D97 residue is located close to other residues previously implicated in glycine and taurine binding. In these mutants, an increase in agonist efficacy coupled with an increase in EC_{50} implies that agonist affinity is decreased.

4. Conclusion

Our data support the notion that the efficacies of ligands for the $\alpha 1$ GlyR are determined by conformational changes that occur within and near the LBD. We hypothesize that disruption of the D97–R119 interaction is an important element in receptor activation and that agonists must break this putative intersubunit bond in order to destabilize the initial shut state and facilitate transitions towards the open state. High efficacy agonists are able to effectively disrupt these intersubunit interactions in WT receptors and subsequently favor channel opening, while partial agonists like taurine cannot effectively promote these disruptions. That said, receptor activation does not exclusively depend on the breakage of an intersubunit bond involving D97; i.e. there must be other interactions in the protein structure that allow for receptors to spend at least some time in desensitized, or shut and activatable states.

5. Experimental Procedures

5.1 - Reagents

All chemicals were obtained from Sigma-Aldrich (St. Louis, MO). *Xenopus laevis* were purchased from Xenopus Express (Homasassa, FL) and housed at 19°C on a 12 hr light:dark cycle. Animals were housed, and surgeries performed, in accordance with AAALAC regulations and under an approved protocol at the University of Texas at Austin.

5.2 - Oocyte isolation and cDNA nuclear injection

Oocytes were surgically removed from *Xenopus laevis* housed at 19°C on a 12hr light/dark cycle. Stage V and VI oocytes were selected and placed in isolation media containing 108 mM NaCl, 1 mM EDTA, 2 mM KCl, and 10 mM HEPES, and forceps were used to manually remove the thecal and epithelial layers. The oocyte follicular layer was removed using a 10 minute exposure to 0.5 mg/ml Sigma type 1A collagenase in buffer containing 83 mM NaCl, 2 mM MgCl₂, and 5 mM HEPES. Injection of a 30 nl sample of the human glycine $\alpha 1$ receptor (accession number X52009) subunit cDNA (1.5 ng/30 nl) in a modified pBK-CMV vector (Mihic et al., 1997) was made into the animal poles of oocytes using a digital micropipette (10 – 15 μ m tip size) attached to a microdispenser. Oocytes were stored in 96-well plates in the dark at 19°C in Modified Barth's Saline (MBS) [88 mM NaCl, 1 mM KCl, 2.4 mM NaHCO₃, 10 mM HEPES, 0.82 mM MgSO₄·7H₂O, 0.33 mM Ca(NO₃)₂, 0.91 mM CaCl₂ at pH 7.5] plus 2 mM sodium pyruvate, 0.5 mM theophylline, 10 U/ml penicillin, 10 mg/l streptomycin, and 50 mg/l gentamycin, sterilized by passage through a 0.22 micron filter. Oocytes expressed GlyR within 24 hours and all electrophysiological measurements were made within 5 days of cDNA injection.

2.3 - Whole-cell oocyte electrophysiological recording

Oocytes were placed in a 100 μ l bath and impaled in the animal poles with two high-resistance (0.5–10 M Ω) glass electrodes filled with 3 M KCl. Using a Warner Instruments OC–725C oocyte-clamp (Hamden, CT), oocytes were voltage-clamped at –70 mV while MBS + 2.5 mM tricaine was perfused over them at a rate of 2 ml/min using a Masterflex USA peristaltic pump (Cole Parmer Instrument Co, Vernon Hills, IL) through 18-gauge

polyethylene tubing. All drug solutions were prepared in MBS + 2.5 mM tricine. Drug applications (5–60 sec) were followed by 5–15 minute washout periods as appropriate.

5.4 - Patch clamp electrophysiology and analysis

Detailed methods and solutions for patch acquisition and analysis can be found in Welsh et al. (2009). Briefly, outside-out patches were held at -80 mV and recordings were made according to standard methods (Hamill et al., 1981). Glycine and taurine were prepared in external solution (100 NaCl, 2 mM KCl, 1 mM $\text{MgCl}_2 \cdot 6\text{H}_2\text{O}$, 10 mM HEPES, 2 mM CaCl_2 at pH 7.4 + 2.5 mM tricine), which also served as the external buffer, before being perfused over outside-out patches. The pipette internal solution contained 88 mM CsCl, 10 mM HEPES, 0.82 mM $\text{MgSO}_4 \cdot 7\text{H}_2\text{O}$, 10 mM EGTA and 0.91 mM CaCl_2 at pH 7.4.

5.5 - Single channel data acquisition and analysis

Single channel data were acquired using an Axopatch 200B amplifier attached to a computer running pClamp ver. 9.2 software (Molecular Devices, Union City, CA). Data were digitized at 100 kHz, low-pass filtered at 10 kHz, and stored on a PC hard drive to be analyzed using the single channel analysis programs in QuB (Qin et al., 2000a,b); version 2.0.0.9 was used for preprocessing and segments were selected by eye that contained clusters of high activity with only one channel present. These portions were then idealized using the segmental-k-means algorithm (SKM) (Qin et al., 2000a,b) with a simple two-state $C \leftrightarrow O$ model. This initial idealization was then fit with multiple exponentials added sequentially to a star model (closed state as the center) using the maximum interval likelihood (MIL) method after imposing a deadtime resolution of 30 μs . Portions of tracings consisting of clusters of single openings were used in analysis; in some cases, where there were brief double openings, they were excised and not used in analysis.

5.6 - Statistics

Experimental values are listed as the mean + standard error. Concentration-response curves used to determine the half-maximal effective agonist concentrations (EC_{50}) were fit using the equation (eq. 1): $y = \text{min} + (\text{max} - \text{min}) / (1 + (x/\text{EC}_{50})^{-\text{Hillslope}})$

Statistical analyses were performed using paired t-tests or one-way or two-way ANOVAs (some repeated measures, as indicated) with Tukey's posthoc comparisons, using Sigmaplot ver. 11 (Systat Software, San Jose, CA).

Supplementary Material

Refer to Web version on PubMed Central for supplementary material.

Acknowledgments

Supported by NIAAA/NIH grants R01AA11525 (to S.J.M), F31AA017802 (to B.T.W.) and F31AA017028 (to M.D.B.)

Abbreviations

β -ABA β -aminobutyric acid

β-AIBA	β -aminoisobutyric acid
GlyR	glycine receptor
LBD	Ligand-binding domain
MBS	Modified Barth's Saline
P_{open}	probability of channel being open
SEM	standard error of the mean
τ	dwel-time
TM	transmembrane
WT	wildtype

References

- Auerbach A. Gating of acetylcholine receptor channels: Brownian motion across a broad transition state. *Proc Natl Acad Sci USA*. 2005; 102:1408–1412. [PubMed: 15665102]
- Beckstead MJ, Phelan R, Trudell JR, Bianchini MJ, Mihic SJ. Anesthetic and ethanol effects on spontaneously opening glycine receptor channels. *J Neurochem*. 2002; 82:1343–1351. [PubMed: 12354281]
- Breje K, van Dijk WJ, Klaassen RV, Schuurmans M, van der Oost J, Smit AB, Sixma TK. Crystal structure of an ACh-binding protein reveals the ligand-binding domain of nicotinic receptors. *Nature*. 2001; 411:269–276. [PubMed: 11357122]
- Cornelison GL, Mihic SJ. Contaminating levels of zinc found in commonly-used labware and buffers affect glycine receptor currents. *Brain Res Bull*. 2014; 100:1–5. [PubMed: 24177173]
- Du J, Lü W, Wu S, Cheng Y, Gouaux E. Glycine receptor mechanism elucidated by electron cryo-microscopy. *Nature*. 2015; 526:224–229. [PubMed: 26344198]
- Ericson M, Molander A, Stomberg R, Söderpalm B. Taurine elevates dopamine levels in the rat nucleus accumbens; antagonism by strychnine. *Eur J Neurosci*. 2006; 23:3225–3229. [PubMed: 16820013]
- Grossman C, Zhou M, Auerbach A. Mapping the conformational wave of acetylcholine receptor channel gating. *Nature*. 2000; 403:773–776. [PubMed: 10693806]
- Grudzinska J, Schemm R, Haeger S, Nicke A, Schmalzing G, Betz H, Laube B. The beta subunit determines the ligand binding properties of synaptic glycine receptors. *Neuron*. 2005; 45:727–739. [PubMed: 15748848]
- Hamill OP, Marty A, Neher E, Sakmann B, Sigworth F. Improved patch-clamp techniques for high-resolution current recordings from cells and cell free membrane patches. *Pflugers Arch*. 1981; 391:85–100. [PubMed: 6270629]
- Huang X, Chen H, Michelsen K, Schneider S, Shaffer PL. Crystal structure of human glycine receptor- α 3 bound to antagonist strychnine. *Nature*. 2015; 526:277–280. [PubMed: 26416729]
- Huxtable RJ. Physiological actions of taurine. *Physiol Rev*. 1992; 72:101–163. [PubMed: 1731369]
- Kuhse J, Betz H, Kirsch J. The inhibitory glycine receptor: architecture, synaptic localization and molecular pathology of a postsynaptic ion-channel complex. *Curr Opin Neurobiol*. 1995; 5:318–323. [PubMed: 7580154]
- Kumar S, Nussinov R. Close-range electrostatic interactions in proteins. *ChemBiochem*. 2002; 3:604–617. [PubMed: 12324994]
- Lape R, Colquhoun D, Sivilotti LG. On the nature of partial agonism in the nicotinic receptor superfamily. *Nature*. 2008; 454:722–727. [PubMed: 18633353]

- Lynch JW. Molecular structure and function of the glycine receptor chloride channel. *Physiol Rev.* 2004; 84:1051–1095. [PubMed: 15383648]
- McCool BA, Botting SK. Characterization of strychnine-sensitive glycine receptors in acutely isolated adult rat basolateral amygdala neurons. *Brain Res.* 2000; 859:341–351. [PubMed: 10719083]
- Mihic SJ, Ye Q, Wick MJ, Koltchine VV, Krasowski MD, Finn SE, Mascia MP, Valenzuela CF, Hanson KK, Greenblatt EP, Harris RA, Harrison NL. Sites of alcohol and volatile anaesthetic action on GABA_A and glycine receptors. *Nature.* 1997; 389:385–389. [PubMed: 9311780]
- Miller PS, Topf M, Smart TG. Mapping a molecular link between allosteric inhibition and activation of the glycine receptor. *Nat Struct Mol Biol.* 2008; 15:1084–1093. [PubMed: 18806798]
- Mori M, Gahwiler BH, Gerber U. β -alanine and taurine as endogenous agonists at glycine receptors in rat hippocampus *in vitro*. *J Physiol.* 2002; 539:191–200. [PubMed: 11850512]
- Qin F, Auerbach A, Sachs F. A direct optimization approach to hidden Markov modeling for single channel kinetics. *Biophys J.* 2000a; 79:1915–1927. [PubMed: 11023897]
- Qin F, Auerbach A, Sachs F. Hidden Markov modeling for single channel kinetics with filtering and correlated noise. *Biophys J.* 2000b; 79:1928–1944. [PubMed: 11023898]
- Schmieden V, Betz H. Pharmacology of the inhibitory glycine receptor: agonist and antagonist actions of amino acids and piperidine carboxylic acid compounds. *Mol Pharmacol.* 1995; 48:919–927. [PubMed: 7476923]
- Schmieden V, Kuhse J, Betz H. Agonist pharmacology of neonatal and adult glycine receptor α subunits: identification of amino acid residues involved in taurine activation. *EMBO J.* 1992; 11:2025–2032. [PubMed: 1376243]
- Schmieden V, Kuhse J, Betz H. A novel domain of the inhibitory glycine receptor determining antagonist efficacies: further evidence for partial agonism resulting from self-inhibition. *Mol Pharmacol.* 1999; 56:464–472. [PubMed: 10462533]
- Todorovic J, Welsh BT, Bertaccini EJ, Trudell JR, Mihic SJ. Disruption of an intersubunit electrostatic bond is a critical step in glycine receptor activation. *Proc Natl Acad Sci USA.* 2010; 107:7987–7992. [PubMed: 20385800]
- Welsh BT, Goldstein BE, Mihic SJ. Single-channel analysis of ethanol enhancement of glycine receptor function. *J Pharmacol Exp Ther.* 2009; 330:198–205. [PubMed: 19380602]

Highlights

- Glycine receptor $\alpha 1$ subunit aspartate-97 (D97) plays a role in ligand efficacy
- Receptors activate spontaneously after D97 mutation to arginine, alanine, glutamate
- D97 glycine receptor mutants can adopt shut, open or desensitized channel states
- Destabilization of the D97-R119 salt bridge increases partial agonist efficacy

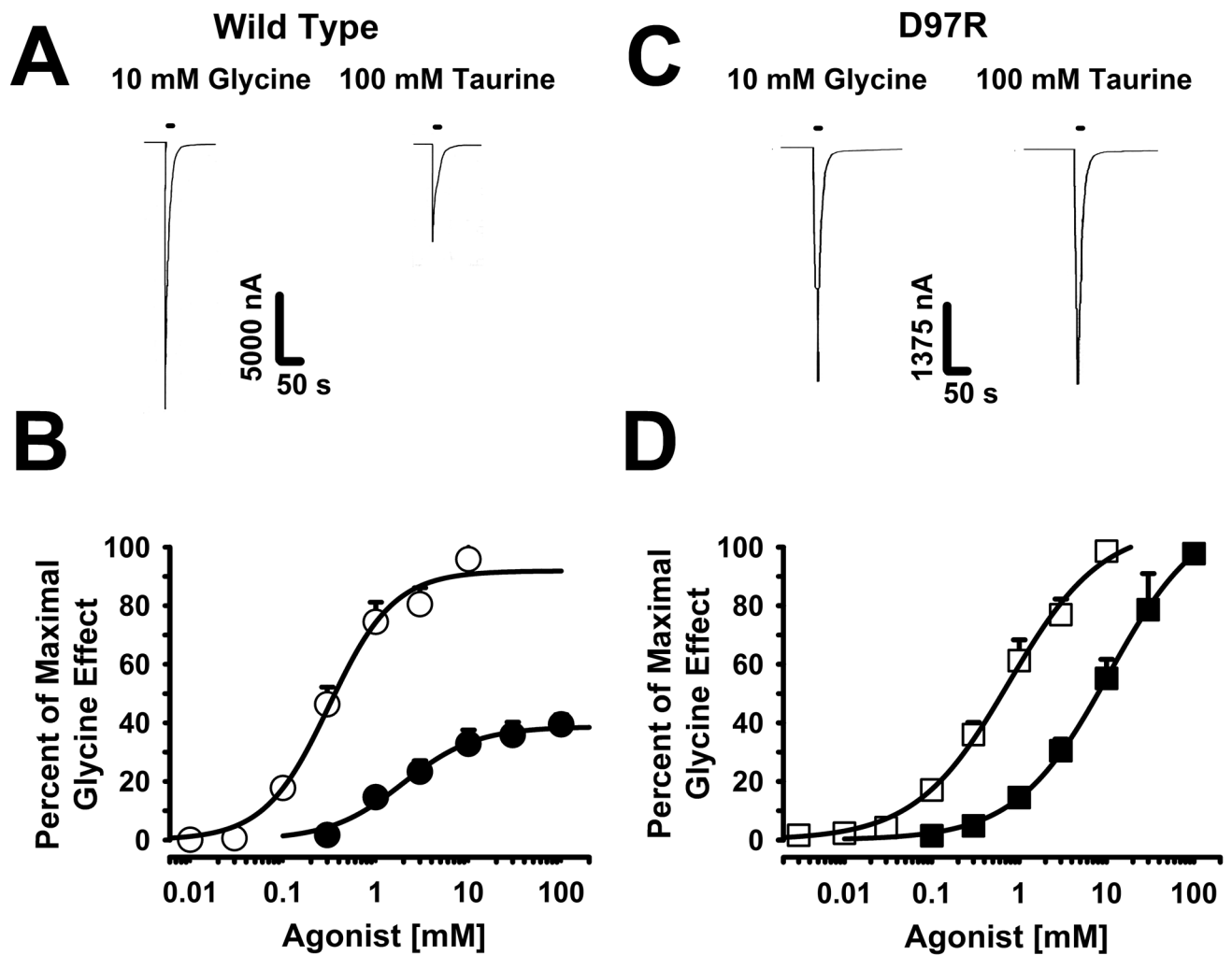


Figure 1. Taurine and glycine elicit currents of similar magnitude on D97R α 1 GlyR
 (A) Representative tracings of whole-cell currents elicited by maximally-effective glycine and taurine concentrations in oocytes expressing WT α 1 GlyR. (B) Whole-cell concentration-response curves for glycine (open symbols) and taurine (filled symbols) tested on WT GlyR. A concentration of 10 mM glycine elicited an average current of $27.6 \pm 2.9 \mu$ A, considerably higher than the $11.8 \pm 1.7 \mu$ A average current elicited by 100 mM taurine [$t(9) = 8.6, p < 0.001$]. (C) Representative tracings of whole-cell currents elicited by maximally-effective glycine and taurine concentrations in oocytes expressing D97R α 1 GlyR. (D) Concentration-response curves for glycine (open symbols) and taurine (filled symbols) applied to D97R α 1 GlyR. A concentration of 10 mM glycine elicited an average current of $3.68 \pm 0.37 \mu$ A, which was not significantly different than the $3.56 \pm 0.36 \mu$ A average current elicited by 100 mM taurine [$t(10) = 1.27, p > 0.23$]. All data point values in graphs 1B and 1D are normalized to the maximal currents obtained with glycine ($I/I_{\max \text{ glycine}}$). An additional experiment comparing the effects of taurine and glycine, tested at concentrations of 300 mM, showed that taurine produced a slightly ($12.7 \pm 7.1\%$) greater current than glycine on D97R α 1 GlyR.

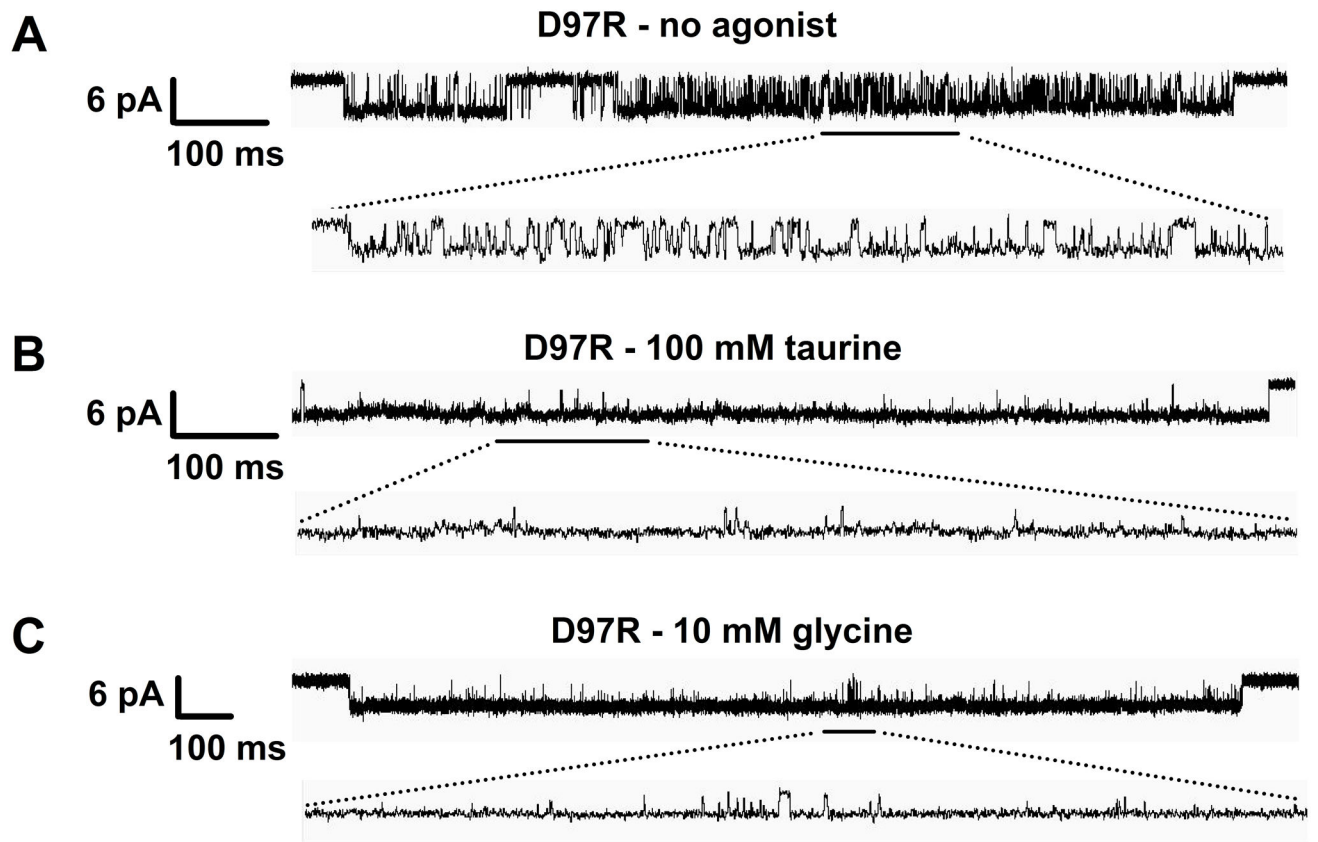


Figure 2. D97R single channel activity in the absence and presence of taurine or glycine
(A) Sample single channel trace obtained from an outside-out patch pulled from an oocyte expressing D97R $\alpha 1$ GlyR in the absence of agonist and in the presence of 2.5 mM tricine. The top tracing shows 1.1 s of recording while the bottom tracing is an expanded view of the section of the top tracing delineated by the horizontal bar. **(B)** Sample trace (1 s in duration) in the presence of 100 mM taurine + 2.5 mM tricine. **(C)** Sample trace (2 s in duration) in the presence of 10 mM glycine + 2.5 mM tricine. Downward deflections indicate channel opening.

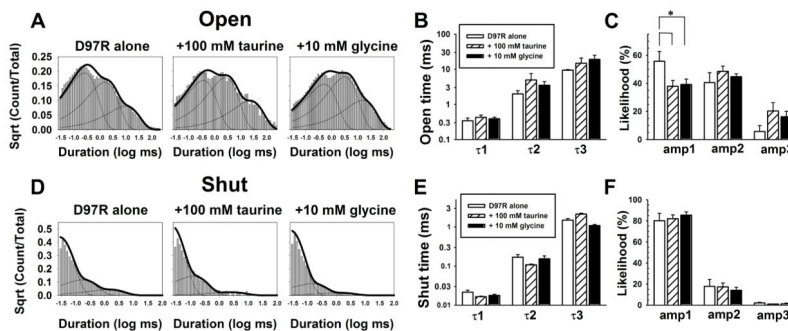


Figure 3. Open and shut dwell time histograms and analysis of single channel opening events in D97R α 1 GlyR

(A) Representative histograms demonstrating the fits of the opendwell times in the absence of agonist, in the presence of 100 mM taurine, or in the presence of 10 mM glycine. The thinner lines in each histogram describe the individual dwell time exponential functions, whereas the thicker line is a fit of all the data. Each condition was fit using three open time components (τ s). (B) Neither agonist affected average durations of open dwell-times compared to the no agonist condition. (C) There was a general effect of likelihood [$F(2,30) = 35.958$, $p < 0.001$]. A Tukey's posthoc test revealed that the no agonist condition differed from taurine and glycine in the shortest likelihood of channel opening, although taurine and glycine did not differ from one another. (D) Representative histograms demonstrating the fits of the shut-dwell times in the absence of agonist, in the presence of 100 mM taurine, or in the presence of 10 mM glycine. The thinner lines in each histogram describe the individual dwell time exponential functions, whereas the thicker line is a fit of all the data. Taurine and glycine had no effects on shut dwell-time components. Each condition was fit using three shut time components (τ s). (E) Neither agonist affected average durations of shut dwell-times compared to the no agonist condition. (F) Neither agonist affected the likelihoods of the shut time components. Data are shown as mean + SEM of 3–5 patches. * indicates a difference at $p < 0.05$.

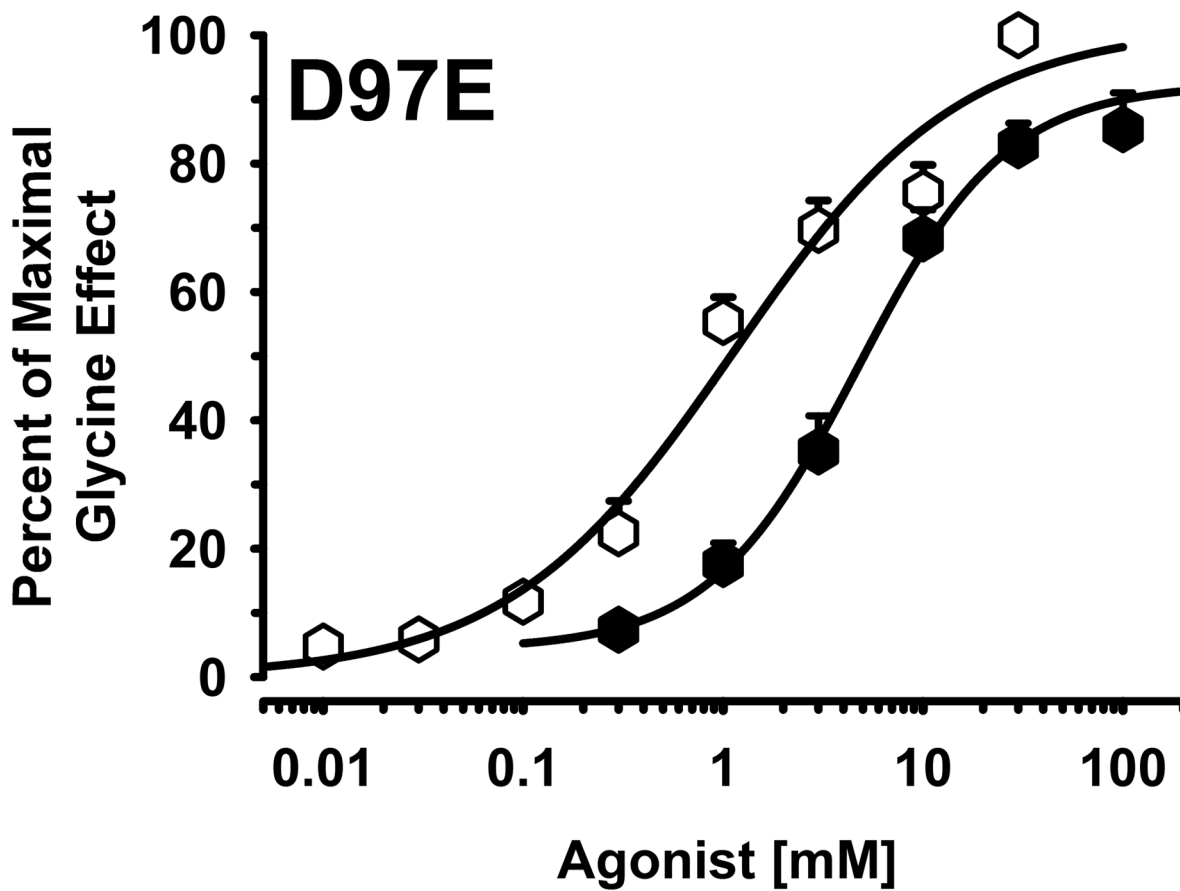


Figure 4. A conservative mutation at D97 (D97E) yields increased taurine efficacy at $\alpha 1$ GlyR Whole-cell concentration-response curves for glycine (open symbols) and taurine (filled symbols) tested on D97E $\alpha 1$ GlyR. A concentration of 10 mM glycine elicited an average current of $11.9 \pm 2.9 \mu\text{A}$, which did not differ from the $11.4 \pm 2.9 \mu\text{A}$ average current elicited by 100 mM taurine [$t(5) = 0.7, p > 0.51$]. All data point values in graphs are normalized to the maximal currents obtained with glycine ($I/I_{\text{max glycine}}$).

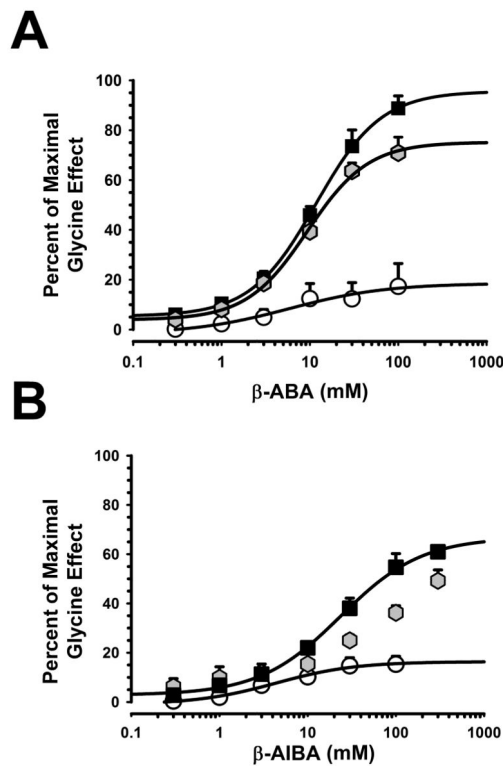


Figure 5. Mutations at D97 increase the efficacies of weak partial agonists

(A) Whole-cell concentration-response curves were generated for β -ABA on WT (open circles), D97E (gray hexagons), and D97R (black squares). One-way ANOVA showed significant differences in the responses to β -ABA on the three receptors [$F(2,9) = 27.8$, $p < 0.001$] and Tukey's post hoc comparisons showed significant differences between β -ABA effects on WT vs D97R and WT vs. D97E, but not D97R vs D97E, responses. (B) Concentration-response curves were generated for β -AIBA on WT (open circles), D97E (gray hexagons), and D97R (black squares). One-way ANOVA showed significant differences in the responses to β -AIBA on the three receptors [$F(2,9) = 53.7$, $p < 0.001$], and Tukey's post hoc comparisons showed significant differences between β -AIBA effects on WT vs D97R and WT vs. D97E, but not D97R vs D97E, responses. All data points are normalized to the maximal currents obtained with 10 mM glycine ($I/I_{\max \text{ glycine}}$). Note: the D97E responses to β -AIBA could not be fit to equation 1 described in Methods.

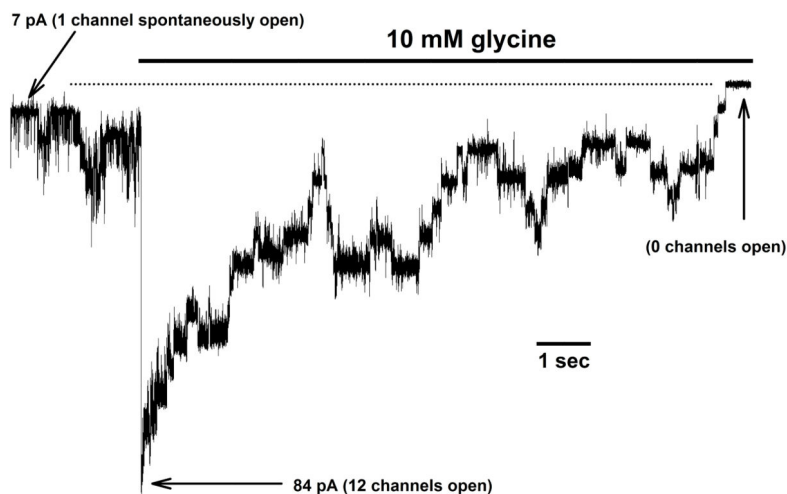


Figure 6. D97A $\alpha 1$ GlyR cycle between shut, spontaneously-active, and desensitized states
In the tracing shown there is initially a single spontaneously-active channel generating 7 pA of current in the absence of agonist. Application of 10 mM glycine activates additional channels, generating a total current of 84 pA. The subsequent decrement in current, eventually to zero, reflects receptor desensitization. The solid horizontal bar represents the time of 10 mM glycine application while the dotted line represents the baseline current observed when all channels in the patch are shut or desensitized. Data in the tracing were filtered at 1 kHz for visualization purposes.

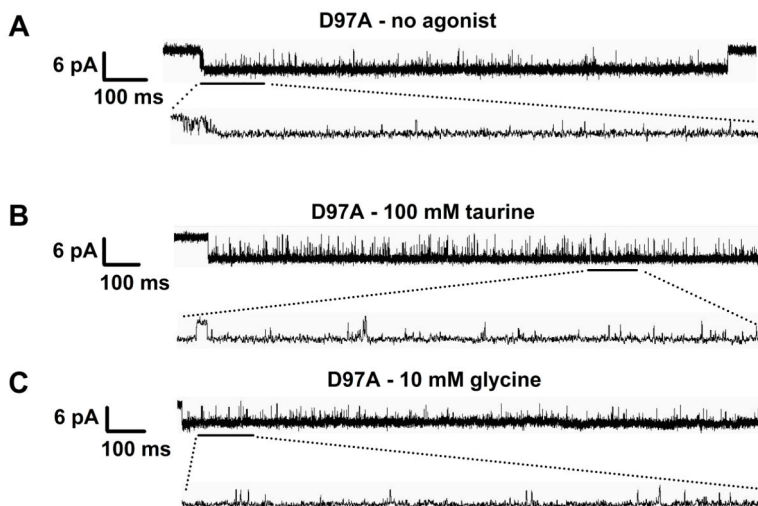


Figure 7. D97A single channel activity in the absence and presence of taurine or glycine
(A) Sample single channel trace obtained from an outside-out patch pulled from an oocyte expressing D97A $\alpha 1$ GlyR in the absence of agonist and in the presence of 2.5 mM tricaine. The top tracing shows 1.4 s of recording while the bottom tracing is an expanded view of the section of the top tracing delineated by the horizontal bar. **(B)** Sample trace (1.7 s in duration) in the presence of 100 mM taurine + 2.5 mM tricaine. **(C)** Sample trace (1.6 s in duration) in the presence of 10 mM glycine + 2.5 mM tricaine. Downward deflections indicate channel opening.

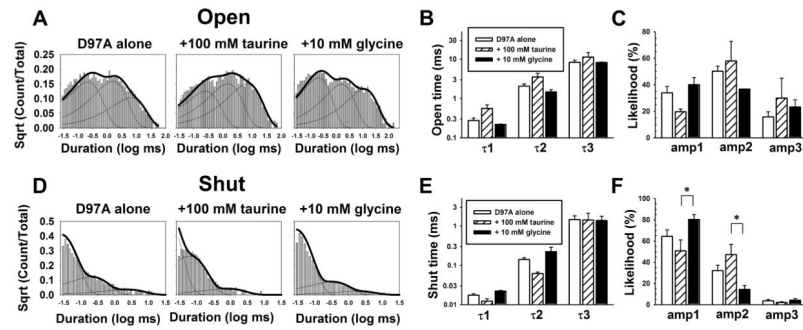


Figure 8. Open and shut dwell time histograms and analysis of single channel opening events in D97A α .1 GlyR

(A) Representative histograms demonstrating the fits of the open dwell times in the absence of agonist, in the presence of 100 mM taurine, or in the presence of 10 mM glycine. The thinner lines in each histogram describe the individual dwell time exponential functions, whereas the thicker line is a fit of all the data. Taurine and glycine had no effects on open dwell-time components. Each condition was fit using three open time components (τ s). (B) Neither agonist significantly affected average durations of open dwelltimes compared to the no agonist condition. (C) Neither agonist affected the likelihoods of occurrence of the open dwell-time components. (D) Representative histograms demonstrating the fits of the shut dwell times in the absence of agonist, in the presence of 100 mM taurine, or in the presence of 10 mM glycine. The thinner lines in each histogram describe the individual dwell time exponential functions, whereas the thicker line is a fit of all the data. Each condition was fit using three shut time components (τ s). (E) Neither agonist affected average durations of shut dwell-times compared to the no agonist condition. (F) There was a general effect of likelihood [$F(2,38) = 85.226$, $p < 0.001$]. A Tukey's posthoc test revealed that taurine and glycine differed in the first and second likelihoods of channel closing, although neither differed from the no agonist condition. Data are shown as mean + SEM of 3–6 patches. * indicates a difference at $p < 0.05$.

Table 1

Ligand	$\alpha 1$ WT (4-6)		D97R (3-7)		D97E (3-6)		D97R/R119E (3-10)	
	EC ₅₀ (nM)	Hill Slope	EC ₅₀ (nM)	Hill Slope	EC ₅₀ (nM)	Hill Slope	EC ₅₀ (nM)	Hill Slope
Glycine	0.3	1.3	0.8	0.8	1.1	0.8	> 300	n.d.
Taurine	2.0	1.1	10.5	0.8	4.7	1.2	> 300	n.d.
β -ABA	5.8	0.8	11.7	1.2	9.4	1.3	n.d.	n.d.
β -AIBA	4.4	1.0	23.7	0.9	n.d.	n.d.	n.d.	n.d.
Imax (% of max glycine)								
Taurine	41.0 \pm 4.5 (10)		97.5 \pm 2.8 (11)		95.6 \pm 4.7 (6)		n.d.	
β -ABA	17.3 \pm 9.2 (4)		88.9 \pm 5.0 (4)		70.9 \pm 6.3 (4)		n.d.	
β -AIBA	15.3 \pm 3.3 (4)		61.0 \pm 1.2 (4)		49.2 \pm 4.4 (4)		n.d.	

Whole-cell responses from oocytes injected with cDNA from each of the mutants listed. The data from each mutant for all agonists were fit with equation 1 listed in the methods. I_{max} values for taurine, β -ABA, and β -AIBA are given as a percentage of maximal glycine current \pm the S.E.M. (n) is the number of oocytes used for the experiments. n.d.: not determined.